Parameters set-up for collision avoidance and smooth motion in 5-axis end milling based on a potential field approach

Virgile Lacharnay, Christophe Tournier, Sylvain Lavernhe

ISBN 978-80-904077-7-0
Proceedings of the 11th International Conference on High Speed Machining
September 11-12, 2014, Prague, Czech Republic

HSM2014-14041

PARAMETERS SET-UP FOR COLLISION AVOIDANCE AND SMOOTH MOTION IN 5-AXIS END MILLING BASED ON A POTENTIAL FIELD APPROACH

V. Lacharnay[1], C. Tournier[1*], S. Lavernhe[1]
[1]École Normale Supérieure de Cachan, LURPA, Cachan, France
*Corresponding author; e-mail: Christophe.tournier@lurpa.ens-cachan.fr

Abstract
Although 5-axis free form surface machining is commonly proposed in CAD/CAM software, collision detection between the tool and the part with smooth tool axis reorientations still need to be addressed. In this paper, a physically based method using potential fields is developed to generate 5-axis collision-free smooth tool paths. The ball-end tool is considered as a rigid body moving in 3D space on which repulsive and attractive forces are acting. Investigations are carried out to set-up the simulation parameters and prevent the tool axis orientation from oscillating and to ensure a smooth behavior.

Keywords:
5-axis machining; collision-free; potential field; tool path generation; ball-end milling

1 INTRODUCTION

5-axis milling is required for the realization of difficult parts such as blades and impellers and is also very convenient to improve quality for the machining of deep molds in plastic injection and casting by reducing tool length. Despite the evolution of CAM software, 5-axis tool path programming requires advanced skills and collision detection remains a challenge during the tool path computation. In the literature numerous papers deal with global collision avoidance in 5-axis milling. Several approaches exist and are based on collision tests executed during the tool path computation or during the post-processing of the tool path.

Methods are usually based on models to represent the tool geometry and the environment (part surface, check surfaces, etc.), a collision test between the obstacle and the tool and finally a correction or optimization of the tool axis orientation to avoid the obstacle. It is during this final stage of optimization that the smoothness of the trajectory may be corrected. Two main approaches exist in the literature, geometric methods, which are the most used, and potential methods. With the geometric approach, the problem is mainly treated in a local coordinate system attached to the tool using the C-Space approach [Choi et al. 1997]. Interferences between the tool and the check surface are detected using algorithms primarily based on surface intersections [Monies et al. 2004]. These tests lead to the definition of a collision free area in the C-Space to orient the tool axis [Morishige et al. 1997]. Another geometric method frequently used to evaluate the interference is based on the cones and maps of visibility. This problem addressed by [Lee et al. 1995] and [Balasubramaniam et al. 2000] enables, using Gaussian sphere, to generate a local visibility map taking into account the part surface and then to integrate the machine constraints accessibility (tool, tool holder, environment) to reduce the space available for the tool axis (global visibility). The final step is the optimization of the tool path in the resulting C-Space collision-free domain including constraints such as smoothness of the tool postures or tool length minimization [Ho et al. 2003],[Bi et al. 2010]. More detail about these approaches to avoid global collisions can be found in [Tang 2014]

The other approach, based on potential fields, has been implemented in the domain of mobile robotics for collision avoidance. This consists in using virtual potential fields that allow a robot to avoid the obstacle during an excessive approach [Khatib 1986]. In addition, taking into account the dynamics [Koren et al. 1991] illustrates the presence of oscillations when the robot moves back towards the programmed position. However, in the field of mobile robotics, this issue is less critical due to the large tolerances allowed on the trajectories.

This approach has already been applied within the context of 5-axis machining for collision avoidance in a static case. Indeed, the work of [Cho et al. 1997] uses a simplified version of the formulation of repulsive forces developed by [Khatib 1986] to treat local and global collisions. The distances between the tool and the part and check surfaces are reformulated into an energy minimization problem to iteratively determine a better tool posture. However, since the proposed approach is quasi-static, i.e. applied from point to point on the trajectory, the appearance of oscillations is a problem raised by the authors themselves.

Thus the aim of this paper is to show the benefit of a dynamic method using potential fields to compute the tool axis orientation along a given tool path. The study focuses more particularly on the set-up of the simulation parameters ensuring collision avoidance and smooth trajectories in 5-axis ball-end milling. This new approach allows in particular to avoid the optimization stage of the tool axis orientation in the collision-free C-Space domain required to ensure the smoothness of the tool path.

The mechanical model of the tool movement computation is presented in the next section. Then simulation parameter values are investigated in section 3. An application on a 5-axis open pocket is carried out in section 4 before the concluding remarks.

2 THE POTENTIAL FIELD APPROACH

2.1 General framework

In the proposed approach, the tool is considered as a rigid body moving in the 3D space on which repulsive and attractive forces are acting. 5-axis collision avoidance is managed thanks to repulsive forces deriving from a potential field

In order to illustrate the effect of repulsive and attractive forces, the tool geometry is reduced to a unique point such as its center of mass *G*, located on the tool axis. However, the tool could be modeled as a set of points *P* which are distributed whether on the tool axis or on the tool surface.

In 5-axis ball-end milling, the tool axis orientation is defined in the local coordinate system (C_L, **f**, **n**, **t**) where C_L is the tool center, **f** the unit vector tangent to the tool path, **n** is the unit vector normal to the part surface and **t** such as **t** = **f** ∧ **n** (Fig.1). In this coordinate system, the tool axis can be rotated around each of the three unit vectors without generating local collision on the active part. In the proposed method, roll angle $(\theta_f, \mathbf{f})$ and pitch angle $(\theta_t, \mathbf{t})$ are used to control the tool axis orientation.

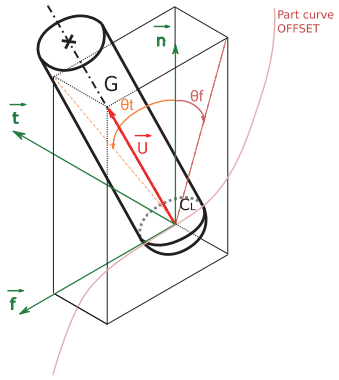

Fig. 1: Tool position an tool orientation set-up

The tool center follows the programmed tool path whereas the tool axis orientation is computed to avoid the obstacles by resolving the fundamental principle of dynamics. Furthermore, the tool velocity along the tool path is supposed to be constant and equal to a value defined by the end user. This principle applied at the center of masse *G* of the tool and expressed in the local frame (C_L, **f**, **n**, **t**), leads to the following equation (Eq.1):

$$\boldsymbol{J}.\frac{d\boldsymbol{\Omega}(t)}{dt} = \boldsymbol{\mathcal{T}}(t) \tag{1}$$

where $\boldsymbol{J}$ is the inertia tensor, $\boldsymbol{\Omega}(t)$, the angular velocity of the tool, which derivates from the angular position θ_f and θ_t within the local frame, $\boldsymbol{\mathcal{T}}$ the total torque. Since the tool axis can spin around the two vectors **f** and **t**, Eq.1 can be split into two separated scalar equations Eq.2 and Eq.3:

$$J_f.\frac{d^2\theta_f(t)}{dt^2} = \mathcal{T}_f(t) \tag{2}$$

$$J_t.\frac{d^2\theta_t(t)}{dt^2} = \mathcal{T}_t(t) \tag{3}$$

Thus the problem of tool axis orientation can be modeled as two independent pendulum systems in two different planes and ordinary differential equation solver is used to compute the tool motion. Once the framework is established, it is necessary to define a model for the repulsive and attractive forces acting on the tool, in order to compute the resulting torque.

2.2 Implementation of the repulsive and attractive forces

Repulsive forces acting on the tool are due to scalar potential attached to the check surfaces. More precisely, each check surface is tessellated into a set of check points which are considered as collision potential sources. In order to ensure collision avoidance between the check surface and the tool, the expression of the scalar potential generated by each check point O_i is the following (Eq.4):

$$\mathcal{U}_{repi} = \begin{cases} \frac{1}{2}.\left(\frac{1}{r_i - r_s} - \frac{1}{r_0}\right)^2, & \text{if } (r_i - r_s) < r_0 \\ 0, & \text{else} \end{cases} \tag{4}$$

with :

- r_i : distance between the considered point *P* of the tool and the given check point O_i
- r_0 : check point neighborhood value (neighborhood sphere radius on Fig.3.
- r_s : security clearance

Given the scalar potential $\mathcal{U}_{repi}$, the repulsive force field $\boldsymbol{\mathcal{F}_{repi}}$ is defined by :

$$\boldsymbol{\mathcal{F}_{repi}} = -\boldsymbol{\nabla}(\mathcal{U}_{repi}) \tag{5}$$

Assuming that $r = (r_i - r_s)$ and $\mathbf{u_i} = \frac{\mathbf{O_iP}}{||\mathbf{O_iP}||}$ this leads to:

$$\boldsymbol{\mathcal{F}_{repi}} = \begin{cases} \left(\frac{1}{r} - \frac{1}{r_0}\right).\frac{1}{r^2}.\mathbf{u_i}, & \text{if } r < r_0 \\ 0, & \text{else} \end{cases} \tag{6}$$

The evolution of $\boldsymbol{\mathcal{F}_{repi}}$ relative to r_i, the distance between the considered point of the tool and the given check point O_i is plotted in Fig.2. The repulsive force tends to infinity when the tool is entering the neighborhood of the check point and becomes closer to it. Collision avoidance is ensured thanks to this behavior.

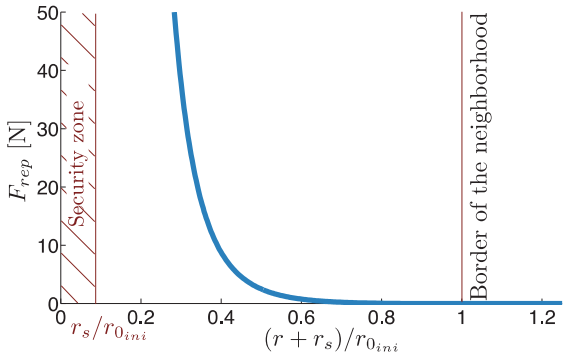

Fig. 2: Repulsive force intensity evolution

Thus, the torque generated at the C_L point by the total repulsive force at each point of the tool P_j is given in Eq.7.

$$\boldsymbol{\mathcal{T}_{rep}} = \sum_{j=1}^{m} \mathbf{C_L P_j} \wedge \boldsymbol{\mathcal{F}_{rep}}(P_j) \tag{7}$$

An attractive torque exerted by a spring is introduced to restore the tool axis orientation in the programmed configuration as well as a viscous damper to allow the system to return to its steady state without oscillating. Thus the additional repulsive and attractive torques lead to the two equations Eq.8 and Eq.9:

$$J_f.\ddot{\theta}_f + c.\dot{\theta}_f + k.(\theta_f - \theta_{fgoal}) = \mathcal{T}_{frep} \tag{8}$$

$$J_t.\ddot{\theta}_t + c.\dot{\theta}_t + k.(\theta_t - \theta_{tgoal}) = \mathcal{T}_{trep} \tag{9}$$

With :

- k : stiffness coefficient
- c : damping coefficient
- θ_{fgoal}: programmed angle around **f**
- θ_{tgoal}: programmed angle around **t**

In these equations, $\mathcal{T}_{frep}$ and $\mathcal{T}_{trep}$ are the projections of the repulsive torque computed at the C_L point in the perpendicular plane to **f** and **t** respectively. The inertia, the damping coefficient and the mass are equal for both equations but they could be different as well, leading to a different behavior in the two planes.

2.3 Transient behavior set-up

When the tool leaves the neighborhood area after avoiding obstacles, it is essential that the tool axis returns in its steady state with a smooth response. In this area, the behavior of the tool axis orientation can be modeled as a damped harmonic oscillator without external applied force. The resulting differential equation is then:

$$J.\ddot{\theta} + c.\dot{\theta} + k.\theta = 0 \tag{10}$$

which can be rewritten into the classic form:

$$\ddot{\theta} + 2.\xi.\omega_0.\dot{\theta} + \omega_0^2.\theta = 0 \tag{11}$$

with:

- $\omega_0 = \sqrt{\frac{k}{J}}$, the natural oscillating frequency
- $\xi = \frac{c}{2.\sqrt{k.J}}$, the damping ratio

Thus, the damping parameter has to be determined according to the next equation relative to a critically damped harmonic oscillator ($\xi \geq 1$):

$$c \geq 2.\sqrt{k.J} \tag{12}$$

where J has been set to 1.

Solving the differential equation without second member ensures a modification of the tool axis orientation with an aperiodic behavior. The second order differential equations with second member corresponding to equations Eq.8 and Eq.9 are not formally resolvable. These equations are thus solved using a differential equation solver as explained hereafter.

3 CONTINUOUS CHECK SURFACE DISCRETIZATION

3.1 Problem definition

Usually, parts encountered in 5-axis milling exhibit continuous check surfaces modeled as parametric surfaces. In order to apply the proposed approach, the check surfaces have to be tessellated and every point of the mesh is considered as a repulsive point whether it belongs to the neighborhood. By applying repulsive and attractive forces as described in the previous section on a rough tessellation of a Bezier patch, the following behavior occurs (Fig.3):

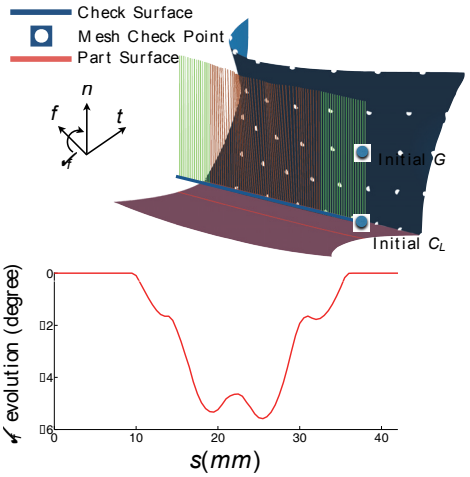

Fig.3: Low density of repulsive points (45 nodes)

The low repulsive point density in the check surface mesh allows the tool to penetrate between the points, thus generating collisions and oscillations. It is therefore important to determine the best tessellation representing the check surface to avoid this type of behavior.

3.2 Steady-state solution analysis

In order to determine the mesh size of the check surfaces to get a smooth response, the influence of points of the obstacle's mesh has to be investigated. The following case study illustrates the worst configuration in terms of steady-state solution. A tool moving along a straight line enters successively different spherical potential fields created by a series of aligned and equally spaced points considered as points of the check surface. The tool geometry is reduced to a unique point located at its center of mass *G*. Before entering the first neighborhood, the orientation of the tool axis is constant, equal to the programmed value. As the tool penetrates in the different neighborhoods, large amplitude oscillations are generated due to the distance between the obstacles (Fig.4). Finally, the tool exits neighborhoods without oscillation respecting the aperiodic response.

To minimize the amplitude of the observed oscillations when the tool enters the different neighborhoods, a driven

harmonic oscillator is considered. The total repulsive force generated by the obstacles is modeled as a sinusoidal driving force such as:

$$\boldsymbol{\mathcal{F}_{rep}} = \boldsymbol{\mathcal{F}_0}.(1+\cos(\omega.t)) \quad (13)$$

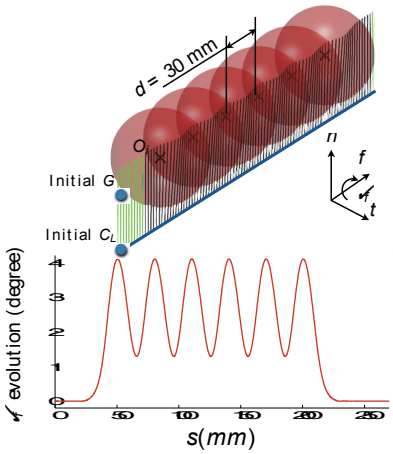

Fig.4: Tool axis behavior with an intermediate distance of 30mm with aligned obstacles

The driving frequency ω of these oscillations depends on the distance d between each obstacle and the velocity v_0 of the tool along the trajectory:

$$\omega = \frac{2.\pi.v_0}{d} \quad (14)$$

Then, the considered differential equation is the following :

$$J.\ddot{\theta} + c.\dot{\theta} + k.\theta = \mathcal{T}_0.(1+\cos(\omega.t)) \quad (15)$$

with:

- $\mathcal{T}_0 = ||\mathcal{F}_0.\mathbf{GC_L}||$

The response is the sum of the transient solution (without second member) $\theta_1(t)$ and the steady-state solution $\theta_2(t)$ with:

$$\theta(t) = \theta_1(t) + \theta_2(t) \quad (16)$$

with :

$$\begin{cases} \theta_1(t) = A_1.e^{-\frac{t}{\tau_1}} + A_2.e^{-\frac{t}{\tau_2}} \\ \theta_2(t) = B.\cos(\omega.t - \Phi) + \frac{\mathcal{T}_0}{k} \end{cases} \quad (17)$$

Regarding the steady-state solution, the amplitude B and the phase Φ are expressed as follows:

$$B = \frac{\mathcal{T}_0/k}{\sqrt{\left(1-\left(\frac{\omega}{\omega_0}\right)^2\right)^2 + 4.\xi^2.\left(\frac{\omega}{\omega_0}\right)^2}} \quad (18)$$

$$\tan(\Phi) = \frac{2.\xi.\left(\frac{\omega}{\omega_0}\right)}{1-\left(\frac{\omega}{\omega_0}\right)^2} \quad (19)$$

The amplitude of the steady-state solution is illustrated on Fig.5 in the case of an aperiodic response with the parameters of Tab.1. Thus, the choice of a driven frequency such as $\left(\frac{\omega}{\omega_0}\right) \rightarrow \infty$ corresponding to the reduction of the distance between the obstacles d along the tool path decreases the amplitude ratio.

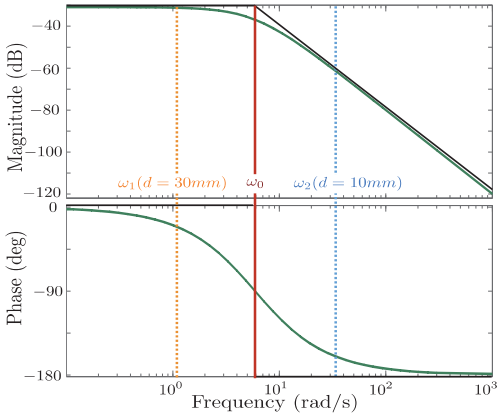

Fig.5: Gain pattern of damped system

Reducing the distance between the obstacles by a factor of 3, $\omega_1 = 3.\omega_2$, leads to a greater attenuation of oscillations as illustrated in Fig.5 and Fig.6. However, oscillations are still visible in accordance with the model. Indeed, the case study is very unfavorable because the tool is reduced to a point so it can penetrate between two consecutive obstacles.

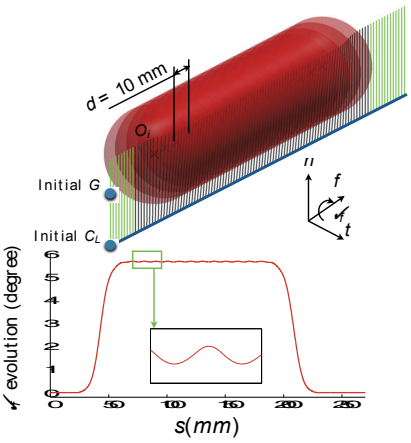

Fig.6: Tool axis behavior with an intermediate distance of 10mm with aligned obstacles

3.3 Application on the Bezier patch

Based on this analysis, the mesh of the considered Bezier patch is densified as illustrated on Fig.(7). The total repulsive force $\boldsymbol{\mathcal{F}_{rep}}$ is plotted as well as the resulting roll angle θ_f. One can then observe that $\boldsymbol{\mathcal{F}_{rep}}$ presents small oscillations in contrast to the smooth evolution of the angle θ_f. Indeed, the mesh nodes of the check surface are sufficiently close and the oscillations are attenuated by the dynamic behavior of the second order system and by the numerical resolution done by the EDO solver. Collision avoidance is respected and the return to the initial programmed orientation is performed without oscillation.

Fig.7 also emphasizes the positive effect of the dynamic approach compared to a static approach. As the differential equation of the tool motion is of second order, the variation of tool axis orientation always starts with tangency continuity even for the worst case which is the step-response. The resulting tool axis motion is smooth and the decay time is visible at the beginning and at the end of the tool path.

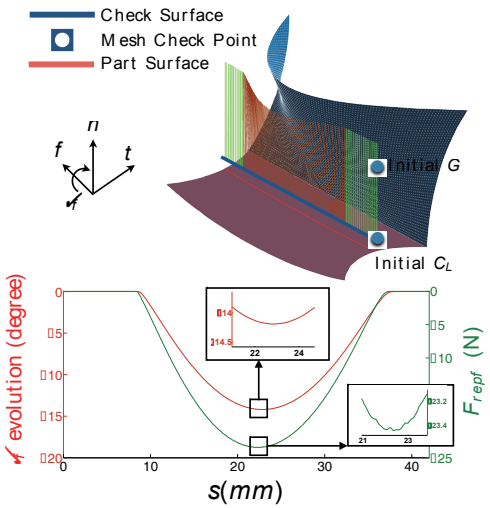

Fig.7: Simulation with a densified mesh (1400 nodes)

Finally, various parameters are at our disposal to prevent oscillations, including the damping parameter and the mesh size of the check surface.

4 APPLICATION

To show the benefit of the proposed approach, the following example deals with the machining of a pocket corner as illustrated in Fig.8 where one can see the planar part surface with the tool location point trajectory as well as the check surface. This is a typical example of mold parts with corners and obstacles that require the use of a 5-axis machining strategy.

In this computation, the total repulsive force $\mathcal{F}_{rep}$ is calculated by summing the forces generated by the mesh points of the check surface. The mesh of the check surface leads to 7803 nodes. The programmed orientation of the tool axis is set normal to the part surface which means $\theta_f = \theta_n = 0$. With such a tool axis orientation strategy, the tool should inevitably collide with the check surface. The ball-end mill radius is equal to 5mm and constant parameters of the computation are listed in Tab.1. Newton's laws are solved using ODE 45, the Ordinary Differential Equation solver proposed in Matlab®.

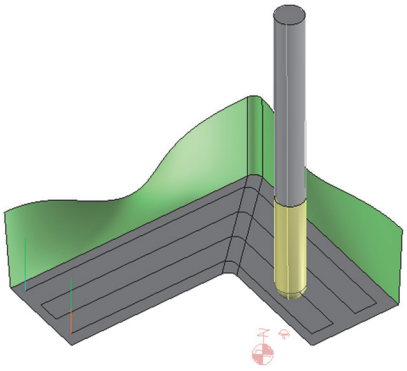

Fig.8: Pocket corner

Computation results are illustrated on figure 9. The feed direction along the tool path is from left to right. The inclined wall of the check surface first modifies the tool axis orientation. Then the tool enters the corner area and especially the neighborhood of the second inclined wall. The tool axis orientation is modified in the corner in a very smooth way. Finally, the tool axis orientation is modified along the second wall and returns in programmed orientation when the tool exists the check surface neighborhood.

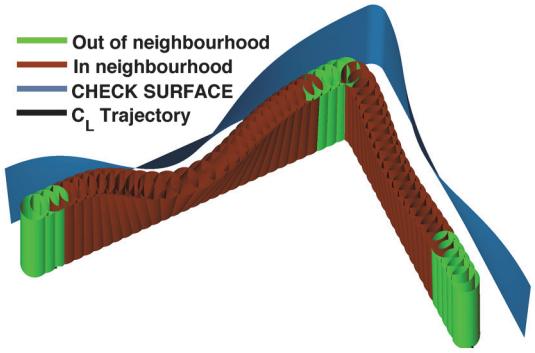

Fig.9: Resulting tool path along the wall

Thus the computation generates a smooth trajectory and the potential collisions with the check surface are avoided. Therefore, the proposed approach provides a good alternative to conventional approaches in the case of 5-axis open pocket parts.

5 CONCLUSIONS

This paper presents an original method for 5-axis collision avoidance between the tool and the check surfaces. A physically based modeling is used to compute a continuous tool motion along the tool path without collision. Furthermore, the use of potential fields allows that no collision will ever occur with the obstacles as the neighborhood emits a repulsive force growing to infinity when the tool gets closer to the obstacle.

As the tool axis orientation behaves like a damped harmonic oscillator, investigations are carried out to set-up the simulation parameters and prevent the tool axis orientation from oscillating and to ensure a smooth behavior. Numerical investigations show that the proposed approach is efficient and does not require advanced CAM programming skills to define the collision free tool path.

6 REFERENCES

[Choi et al. 1997] Choi B.K., Kim D.H. and Jerard R.B. C-Space approach to tool-path generation for die and mould machining. Computer-Aided Design 1997; 29(9):657-669.

[Monies et al. 2004] Monies F., Mousseigne M., Redonnet J. M. and Rubio W. Determining a collision-free domain for the tool in five-axis machining. International Journal of Production Research 2004, 42(21):4513-4530.

[Morishige et al. 1997] Morishige K., Kase K. and Takeuchi Y. Collision-Free Tool Path Generation Using 2-Dimensional C-Space for 5-Axis Control Machining. International Journal of Advanced Manufacturing Technology 1997; 13:393- 400.

[Lee et al. 1995] Lee Y-S. and Chang T-C. 2-Phase approach to global tool interference avoidance in 5-axis machining. Computer-Aided Design 1995; 27(10):715-729.

[Balasubramaniam et al. 2000] Balasubramaniam M., Laxmiprasad P., Sarma S. and Shaikh Z. Generating 5-axis NC roughing paths directly from a tesselated representation. Computer-Aided Design 2000; 32(4):261-277.

[Ho et al. 2003] Ho M-C., Hwang H-R. and Hu C-H. Five-axis tool orientation smoothing using quaternion interpolation algorithm. International Journal of Machine Tools & Manufacture 2003; 43:1259-1267.

[Bi et al. 2010] Bi Q. Z., Wang Y. H., Zhu L. M. and Ding H. Generating collision-free tool orientations for 5-axis nc machining with a short ball-end cutter. International Journal of Production Research 2010; 48(24):7337-7356.

[Khatib 1986] Khatib O. Real-Time Obstacle Avoidance for Manipulators and Mobile Robots. The International Journal of Robotics Research 1986; 5(1):90- 98.

[Koren et al. 1991] Koren Y. and Borenstein J. Potential field methods and their inherent limitations for mobile robot navigation. IEEE Transactions on robotics and automation 1991; 1398-1404.

[Cho et al. 1997] Cho I., Lee K. and Kim J. Generation of Collision-Free Cutter Location Data in Five-Axis Milling Using the Potential Energy Method. International Journal of Advanced Manufacturing Technology 1997; 13:523-529.

[Tang 2014] Tran D. T., Algorithms for collision detection and avoidance for five-axis NC machining: A state of the art review, Computer-Aided Design 2014 ; 51:1-17,

Tab.1: Parameters table

Parameters	**Symbol**	**Value**
Tool radius $[m]$	R	$2.5.10^{-3}$
Tool cylinder height $[m]$	H	20.10^{-3}
Tool Inertia $[kg.m^2]$	J	1
C_LCurvilinear speed $[m.s^{-1}]$	v_f	$1/60$
Neighborhood value $[m]$	r_0	13.10^{-3}
Stiffness coefficient $[N.m.rad^{-1}]$	k	32
Damping ratio (no unit)	ξ	1
Programmed initial angle $[rad]$	θ_{goal}	0
Mesh size $[m]$	MS	2.10^{-3}